Metallosupramolecular Zippers Generated by Self-Organization of Self-Complementary Molecular Clefts

Mihail Barboiu,*[a] Eddy Petit,[a] and Gavin Vaughan[b]

Dedicated to Professor Constantin Luca on the occasion of his 73rd birthday

Abstract: The binding of Co^{2+} and Pb^{2+} ions to the terpyridine and pyridine subunits of the ligand **1** leads to the self-complementary molecular clefts **2**–**6**, which result from the crossover combination of orthogonal-terpyridine and linear-pyridine metal-coordination subprograms and are stabilized by strong π–π stacking interactions. Four different cleft-type entities, $[Co^{2+}{}_2(\mathbf{1})_2]$ (**3**), $[Pb^{2+}{}_2(\mathbf{1})_2]$ (**4**), $[Co^{2+}{}_4(\mathbf{1})_2]$ (**5**), $[Pb^{2+}{}_4(\mathbf{1})_2]$ (**6**), are generated in both solution and the solid state, and may be interconverted as a function of metal/ligand stoichiometry. One- and two-dimensional metallosupramolecular zipper architectures result from self-assembly in the solid state driven by a combination of different π–π stacking subprograms. The U-shaped geometry of the ligand influences the possibility of zipping and thus, in turn, the generation of different zipper architectures. The structures of **2**–**5** have been confirmed by X-ray crystallography; that of **6** is based on NMR spectral data.

Keywords: cleft structures · cobalt · lead · N ligands · supramolecular chemistry · zippers

Introduction

Within supramolecular chemistry, the use of functional supramolecular architectures to act as constitutionally dynamic adaptative materials, has emerged as a major field of with the goal of designing self-organizing nanosystems of increasing complexity.[1–3] The self-assembly of coordination-based entities is based on the implementation of ligands that contain specific molecular information stored in the arrangement of suitable binding sites and of metal ions reading out the structural information through the algorithm defined by their coordination geometry.[2,3]

Of special interest are ligand systems that contain different binding units within their structure so as to combine several distinct coordination subprograms.[3] Square $[M^{2+}{}_{n^2}(n\times n)]$, $n=2,3,4$ grid-type assemblies based on terpyridine subunits and octahedrally coordinated metal ions have been actively studied by Lehn et al.[6] Different three-dimensional superstructures assembled through pyridine–metal coordination reported by the groups of Stang[2a,d] and Fujita,[2e] reveal a range of interesting structural and physicochemical properties.

The ligand **1** discussed in this paper operates under conditions in which available terpyridine (terpy) and pyridine (py) coordination sites can be involved in the orthogonal[4] and linear[5] (Scheme 1) binding events, respectively, of the octahedral metal ions. Specifically, it is of interest to investi-

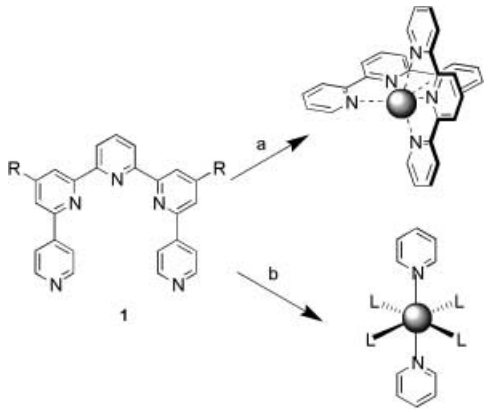

Scheme 1. Ion-coordination subprograms encoded in the structure of ligand **1**: a) orthogonal-terpyridine and b) linear-pyridine binding events of the metal ions. R = –S*n*Pr.

[a] Dr. M. Barboiu, E. Petit
Institut Européen des Membranes, IEM-CNRS 5635
Place Eugène Bataillon, CC 47
34095 Montpellier, Cedex 5 (France)
Fax: (+33) 467-14-91-19
E-mail: barboiu@iemm.univ-montp2.fr

[b] Dr. G. Vaughan
European Synchrotron Radiation Facility
BP 220, 38043 Grenoble Cedex (France)

Supporting information for this article is available on the WWW under http://www.chemeurj.org/ or from the author.

 DOI: 10.1002/chem.200305750

gate whether the coordination behavior of this system, on the addition of octahedral metal ions, could be selectively expressed as an independent (linear) or interfering (crossover) combination of the above binding events, depending on the experimental conditions, such as metal ion concentration, molar ratio, and so forth.

We describe here a study of the equilibrium binding of Co^{2+} and Pb^{2+} ions to the tritopic ligand **1**, which lead to the formation of coordination compounds **2**–**6**. We report the crystal structures of three such complexes **2**–**5**, which assemble into complementary duplex cleft-type compounds, and further self-organize into metallosupramolecular zippers in the solid state.

Result and Discussion

Synthesis and characterization of ligand 1: Ligand **1** was synthesized by means of Potts' methodology[7]: repetitive twofold reaction of the central pyridine bis-Michael acceptor unit **7** with two 4-acetyl-pyridine building blocks **8** to yield **1** (54%) (Scheme 2).

A solution of **1** in $CDCl_3$ gives a sharp ^1H NMR spectrum with strong deshielding of *meta*-protons of the central pyridine ring, consistent with the *transoid*, *transoid* conformation[8] of the ligand (Scheme 2). As expected a strong deshielding is observed for *meta*-pyridine hydrogen atoms, indicating a tight contact with the neighboring pyridine nitrogen atoms; this effect agrees with an unwrapped linear conformation of compound **1**.

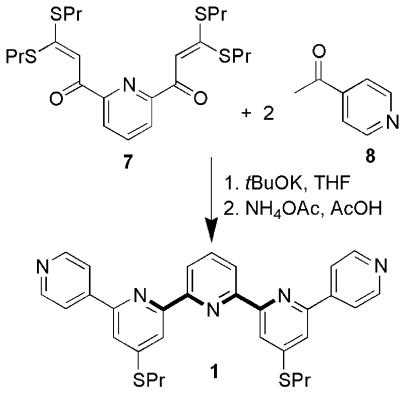

Scheme 2. Reaction sequence for the preparation of ligand **1**

Abstract in Romanian: *Coordinarea cationilor de Co^{2+} si de Pb^{2+} la gruparile terpiridina si piridina a ligandului **1** conduce la formarea de "chei moleculare" auto-complementare **2**–**6** ca urmarea combinarii incrucisate a subprogramelor de coordinare ortogonal (terpyridina) si linear (piridina) si a stabilizarii prin interactii aromatice π-π. Patru entitati diferite $[Co^{2+}{}_2(\mathbf{1})_2]$ (**3**), $[Pb^{2+}{}_2(\mathbf{1})_2]$ (**4**), $[Co^{2+}{}_4(\mathbf{1})_2]$ (**5**), $[Pb^{2+}{}_4(\mathbf{1})_2]$ (**6**), sunt generate atat in solutie cat si in stare solida, care pot fi transformate reciproc in functie de stoiechimetria metal/ligand. Se pot obtine astfel in stare solida, arhitecturi de tip "fermoar" mono si bidimensionale prin combinarea de diferite subprograme de interactiune π–π. Geometria in forma de U a ligandului influenteaza posibilitatea de assamblare si deci conduce la generarea de arhitecturi "fermoar" diferite. Structurile π–π au fost confirmate prin cristalografie de raze X iar cea a compusului **6** prin spectroscopie RMN.*

Controlled generation and interconversion of the Co^{2+} and Pb^{2+} complexes formed by ligand 1: The ability of a ligand such as **1** to form different metal complexes combining different coordination subprograms creates the possibility of forming a diverse set of output coordination devices. The ability to control the generation and interconversion of these entities provides, in principle, a means for taking full advantage of the dynamic constitutional/combinatorial diversity that they offer.[1] Such was the case in the interconversion of arrays of silver(I) ions in the course of the formation of a $[3\times3]$[9] and $[4\times4]$[6d] grids, as well as in the medium-induced adaptive exchange between a square and an hexagonal arrangement of copper(II) ions.[10] Furthermore, in order to control the generation of such supramolecular architectures it is necessary to develop methods for their self-assembly as well as to determine their domains of stability. As a step towards this goal we decided to investigate the formation, existence domain, and interconversion of the polynuclear complexes that may result from the binding of Co^{2+} or of Pb^{2+} ions to various stoichiometric ratios of ligand **1**. Such systems form by self-assembly under mild conditions and are readily amenable to solution studies by

ES mass spectrometry and NMR spectroscopy: ^1H NMR titration was also performed on solutions of $Pb(CF_3SO_3)_2$ and **1** in $[D_3]$acetonitrile. ES mass spectrometry was used to follow the titration of a solution of **1** by a solution of $Co(BF_4)_2$ (Figure 1a) or $Pb(CF_3SO_3)_2$ (Figure 1b) in acetonitrile in order to obtain information about the coordination behavior of **1** towards Co^{2+} or Pb^{2+} ions. Initial complexation studies revealed that addition of $Co(BF_4)_2$ or $Pb(CF_3SO_3)_2$ to a suspension of **1** in acetonitrile caused a rapid dissolution of the ligand in a $\mathbf{1}/M^{2+}$ ($M^{2+}=Co^{2+}$ or Pb^{2+}) molar ratio from 1:0.5 to 1:3. At a $\mathbf{1}/M^{2+}$ ratio of 1:0.5 the ES mass spectra were consistent with the presence of the complex $[Co(\mathbf{1})_2]^{2+}$ (**2**: $m/z=565$) and with the direct formation of $[Pb_2(\mathbf{1})_2(CF_3SO_3)_2]^{2+}$ (**4**: $m/z=892$). Further addition of Co^{2+} ions led to the progressive conversion of **2** into the complex $[Co_2(\mathbf{1})_2(CH_3CN)_4]^{4+}$ (**3**: $m/z=339$), which was the only species present at the required $\mathbf{1}/Co^{2+}$ ratio of 1/1. The charge states of these ions were determined by isotopic profile simulations, which corresponded to symmetrical above-mentioned solvated cations (see Supporting Informations).

Below a $\mathbf{1}/Pb^{2+}$ ratio of 1:1 the ^1H NMR spectra consisted of the exchange-broadened signals of complex **4**, indicative of the slow exchange with the ligand **1** in solution (Figure 1e). At a $\mathbf{1}/Pb^{2+}$ ration of 1:1 the ^1H NMR spectrum of **4** consisted of a series of sharp peaks, indicating high symmetry. The spectra could be interpreted as ligand **1** in one magnetic environment and showed a deshielding of protons of the terpyridine due to the lead ion complexation. Triden-

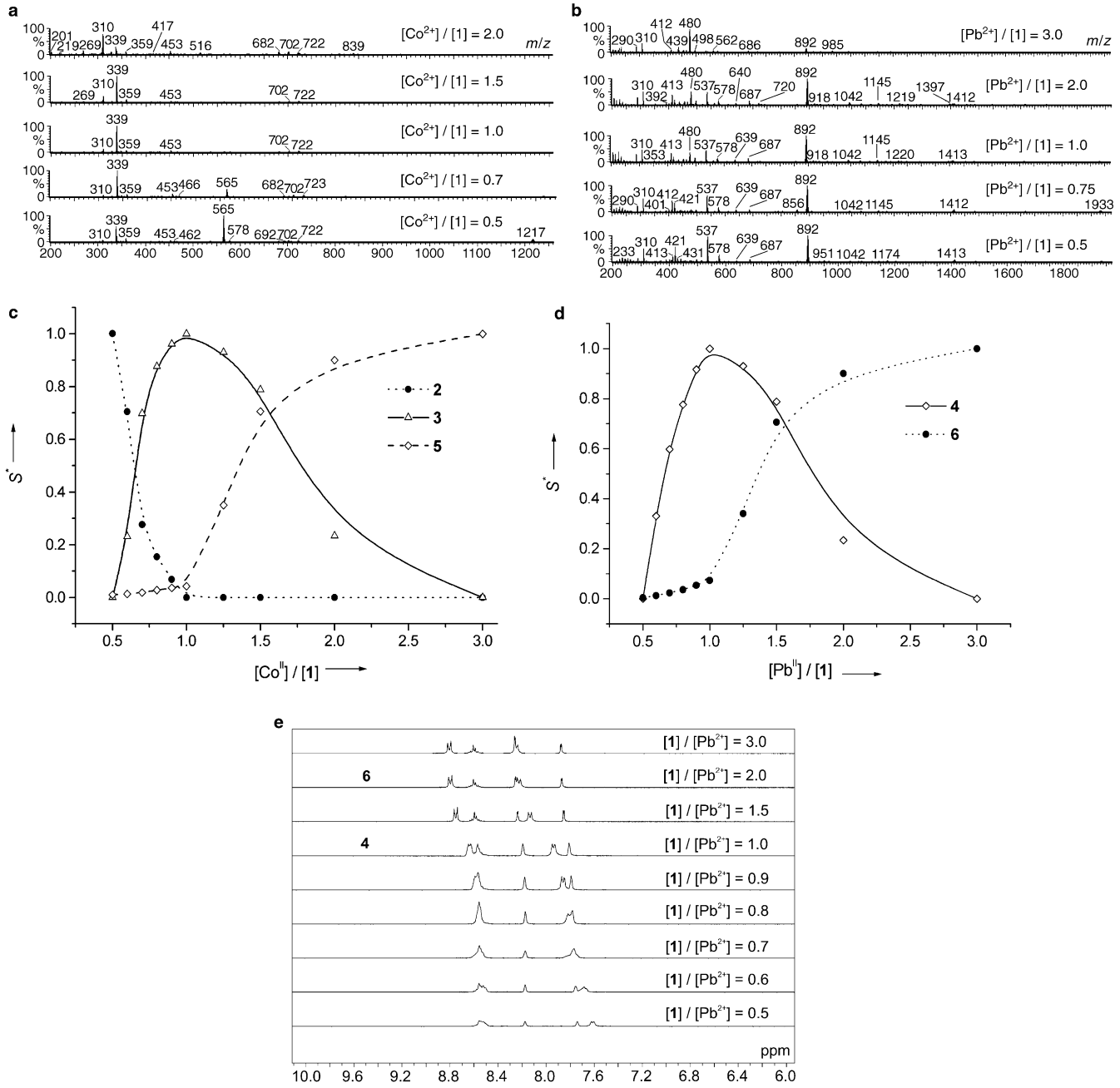

Figure 1. ESI mass spectra and distribution curves of the species resulted on the titration of a solution of ligand **1** in CH_3CN by a solution of M^{2+} in CH_3CN (at initial ligand **1** concentration of 0.002 M) of: a), c) the Co^{2+} complexes **2** (△), **3** (Δ), and **5** (◇); b), d) the Pb^{2+} complexes **4** (◇) and **6** (○). The data points were plotted using the integral surface of characteristic MS-chromatogram peaks normalized by the maximal surface; e) ^{1}H NMR titration experiment of **1** with $Pb(CF_3SO_3)_2$ in CD_3CN.

tate metal ion coordination converts the *transoid*, *transoid* form of the free ligand to *cisoid*, *cisoid* one, corresponding to a terpyridine-type complexation site. The terminal pyridine signals were overall strongly shielded ($\Delta\delta = 1$ ppm) with respect to the ligand **1**, suggesting that intermolecular π–π stacking interactions played an important role in the aggregation process of these compounds.

When the **1**/M^{2+} ratio was increased from 1:1 to 1:3 the duplex complexes **3** and **4** were progressively converted into the new compounds $[Co_4(\mathbf{1})_2(CH_3CN)_{14}(BF_4)_4]^{4+}$ (**5**: $m/z =$ 310) and $[Pb_4(\mathbf{1})_2(CF_3SO_3)_4(CH_3CN)_4]^{4+}$ (**6**: $m/z = 480$) (Scheme 3). The ^{1}H NMR spectrum of **6** indicates the same conformational symmetry of the ligand and, with respect to the complex **4**, shows an overall deshielding of protons of the terpyridine and terminal pyridine moieties due to the subsequent metal ion complexation.

The ES mass and NMR spectroscopic results allow the following conclusions to be drawn:

1) Anticipating the crystal structure results below, all these spectroscopic data agree with the formulation in acetonitrile of the self-complementary duplex cleft structures **3**

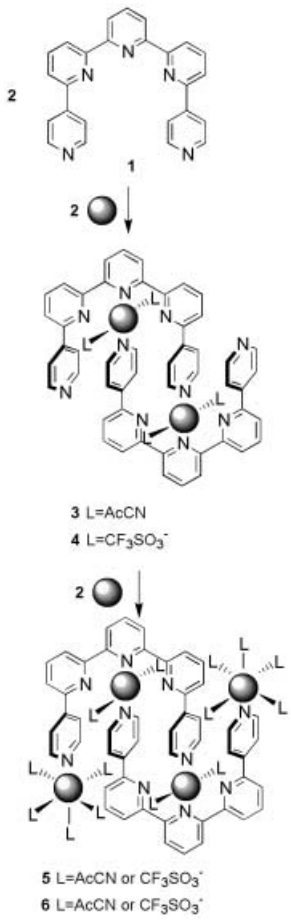

Scheme 3. Reaction sequence for the preparation of complexes **3**–**6**. The S*n*Pr groups were omitted for clarity.

and **5**: the pyridine side wall of one clip molecule filling the cavity of the other and vice versa.

2) These duplex cleft structures are highly robust as they are still preserved even in the presence of a large excess of metal ions (up to 1:3 ligand/ion ratio), despite the presence of several unoccupied ion-binding sites. The same is indicated by the unchanged proton NMR spectra for **3**–**6** at $+60\,^{\circ}C$.
3) The distribution curves of the complexes **2**–**6** generated in the course of the titration of ligand **1** with M^{2+} are shown in Figure 1. The duplex cleft complexes **3** and **4** are formed exclusively, but require that the correct stoichiometry be used. However an intermediate complex **2** was detected in equilibrium with the more stable complex **3**: approximately 80% of **3** is present at a $1/Co^{2+}$ ratio of 1:0.75. Conversely the duplex cleft complexes **3** and **4** are quite robust, remaining quasi-unperturbed on addition of metal ions up to a $\mathbf{1}/M^{2+}$ ratio of 1:1.5. They transform to similar duplex cleft-type complexes **5** and **6** which remain imperturbed on addition of metal ions beyond the required stoichiometry.

Solid-state structures of the M^{2+} (Co^{2+} Pb^{2+}) cleft-type complexes 3, 4, and 5 formed by ligand 1: The crystal structures of the complexes **3**, **4**, and **5**, formed by ligand **1** with Co^{2+} or Pb^{2+} ions, were determined from crystals obtained from solutions in acetonitrile/benzene (1:1) at room temperature.

*Architectures of the duplex cleft-type complexes **3**, **4**, and **5***: The X-ray structural determinations of single-crystals of **3** (pink), **4** (pale-yellow), and **5** (red) reveled that the complexes have approximately the same structure. Self-complementary duplex clefts, which self-assemble in the solid state as intriguing coordination polymers with a unprecedented architecture resulting from the crossover of the orthogonal-terpyridine and the linear-pyridine Co^{2+} or Pb^{2+} complexation subprograms. The molecular and the crystal-packing structures are presented in Figures 2–4.

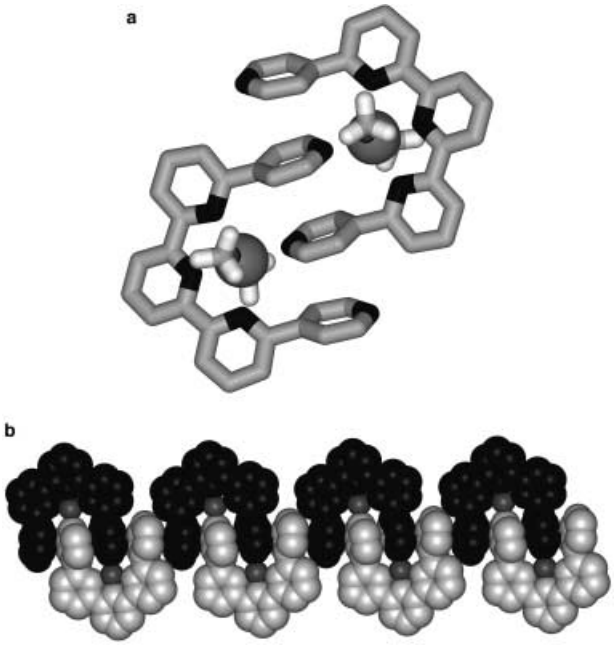

Figure 2. Crystal structure of the duplex cleft complex **3**: a) side view in stick representation; b) space-filling representation of the crystal packing. The cobalt ions are shown as gray spheres.

The unit cell of **3** was found to contain four $[Co^{2+}{}_2(\mathbf{1})_2]$ dimers, forming two stacks, together with eight tetrafluoroborate couterions, 16 coordinated acetonitrile and two benzene molecules. The unit cell of **4** was found to contain one $[Pb^{2+}{}_2(\mathbf{1})_2]$ dimer, together with four triflate counterions and eight uncoordinated acetonitrile molecules. The unit cell of **5** was found to contain four $[Co^{2+}{}_4(\mathbf{1})_2]$ dimers forming two stacks, together with 32 tetrafluoroborate counterions, 16 water and 40 coordinated acetonitrile molecules.

In all structures **3**–**5** the two ligands **1** and two M^{2+} (Co^{2+}, Pb^{2+}) ions form a dimeric self-complimentary molecular cleft, with each $[M^{2+}(\mathbf{1})]$ entity being slotted into the other (Figures 2–4). The cobalt and lead cations are coordinated by one terpy unit of one ligand (the average Co^{2+}–N and Pb^{2+}–N distances are 2.20 Å and 2.55 Å, respectively) and by the inner pyridine arm of the other ligand (the average Co^{2+}–N and Pb^{2+}–N distances are 2.11 Å and 2.93 Å, re-

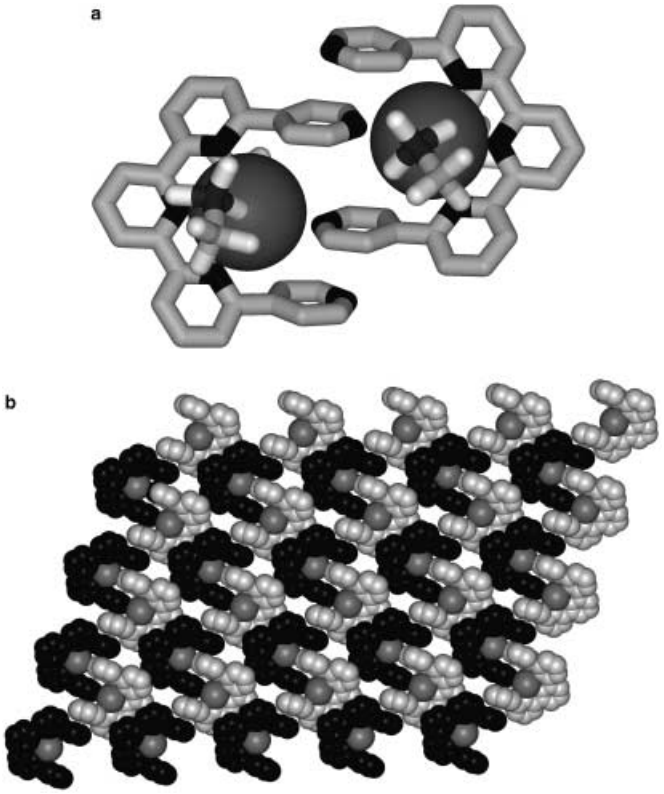

Figure 3. Crystal structure of the duplex cleft complex **4**: a) side view in stick representation; b) space-filling representation of the crystal packing. The lead ions are shown as gray spheres.

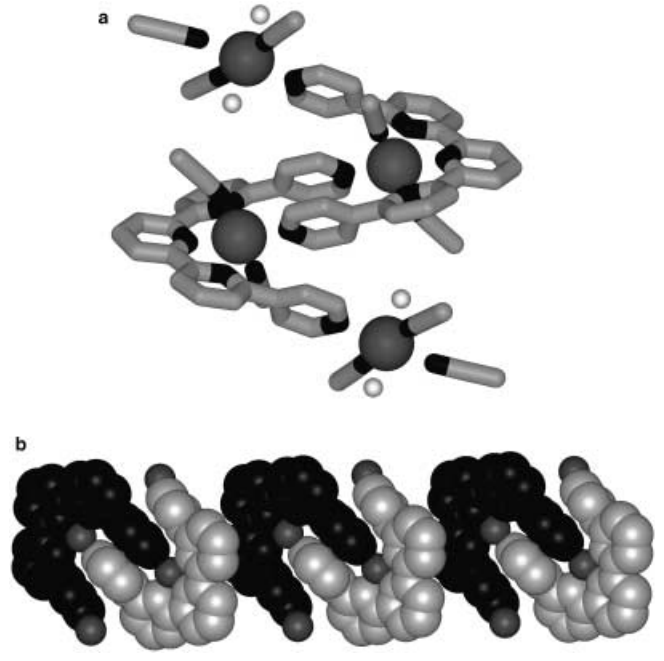

Figure 4. Crystal structure of the duplex cleft complex **5**: a) side view in stick representation; b) space-filling representation of the crystal packing. The cobalt ions are shown as gray spheres.

spectively). The cobalt(II) and lead(II) cations have an octahedral coordination geometry, each open face being occupied by two coordinated acetonitrile molecules (the average Co^{2+}–NCAc distance is 2.15 Å) or by two coordinated triflate counterions (the average Pb^{2+}–OSO_2CF_3 distance is 2.55 Å) (Figures 2a and 3a). The cleft-type structure **3** is preserved in the structure **5**, which is composed of four Co^{2+} ions and two ligands **1**. The octahedral Co^{2+} ions exist in two different distorted geometries: the inner two cleft-structuring Co^{2+} ions possess the same donor sets Co(Terpy:Py:$AcCN_2$) as in the complex **3**. The outer two Co^{2+} are ligated by the second pyridine side arm, three acetonitrile and two water molecules (the average Co^{2+}–OH_2 distance is 2.08 Å) (Figure 4a).

The formation of the self-complementary molecular clefts **3** and **4** imposes an important deviation of the terminal pyridine units from their preferred planar conformation (the Py–Py torsional angles lie within $\sim 52.3 \pm 0.4°$). In this way two inner M^{2+}-complexed and two outer uncomplexed pyridine side arms are situated in a face-to-face stacking arrangement, allowing considerable overlap with average π–π stacking centroid–centroid distances of 3.40 Å (**3**) and 3.73 Å (**4**), corresponding to a strong van der Waals contact compared with other similar systems.[11a] These complexes are stabilized by favorable dipole-complexation/induced-dipole (Figures 2a and 3a) electrostatic interactions between π-donating and π-accepting nitrogen-containing ring systems, which generate a linear compact π–π stacking subset of four overlapping aromatic rings. Subsequent complexation of each external pyridine lateral arm by the Co^{2+} ions allow the conservation of a distorted two by two π–π stacked subset in complex **5**. In this complex the centroid–centroid distance between inner and outer pyridines is 3.60 Å, corresponding to an offset angle of 24.7°, significantly opened up with the respect to those in the structure of **3** (offset angle of 10.2°). These π–π stacking interactions are reminiscent of those observed in the complementary double-helix entities reported earlier[11b] and of the solid-state structures of silver(I) molecular clefts described by McMorran et al.[12]

These cleft-type structures are highly regular and may be propagated in one or two directions without any structural modification by taking advantage of the π–π stacking interactions of the two aromatic components (the terpyridine and the terminal pyridines) of the duplex. In the crystals, each duplex of **3** or **5** has a tight contact with the two neighboring ones by stacking with opposite orientations of the outer pyridine side arms (average distance of 3.87 Å and offset angle of about 10.2°: Figure 2b) or the terpyridine moieties (average distance of 3.70 Å and offset angle of about 10.4°: Figure 4b). The duplex cleft-type structure $\mathbf{1}_2Pb^{2+}{}_2$, **4** combines these two π-π stacking subprograms, each $\mathbf{1}_2Pb^{2+}{}_2$ entity presenting a tight contact with four neighboring ones: two by stacking of the outer pyridine side arms (the average distance of 3.70 Å and the offset angle of about 11.7°) and two by stacking of the terpyridine moieties (the average distance of 4.00 Å and the offset angle of about 9.7°). In the crystal lattices of **3** and **5**, one-dimensional ribbons, as well as and the two-dimensional sheets of **4**, pack into parallel layers that are alternatively stratified above one another in an ABAB arrangement. The layers are connected by an additional interaction between the

−S*n*Pr moieties of each alternate layer. The anions, acetonitrile, benzene, and water molecules fill the interstices between the complex cations in **3**–**5**.

The X-ray crystallographic results allow the following conclusions to be made:

1 In terms of molecular programming the cleft-type architectures **3**, **4**, and **5** represent attractive arrays of cobalt and lead ions: sets of ion dots[6c,13] of well-defined arrangements accessible in a single operational step by the crossover combination of distinct metal-coordination programs and stabilized by strong π–π stacking interactions.

2) In terms of programmed self-assembly, the self-complementary molecular clefts self-organize in the solid state in metallosupramolecular one- and two-dimensional zippers of stacked duplexes, which are positioned with respect to one another as a function of two π–π stacking subprograms: one dimensional a) pyridine-π–π stacked and b) terpyridine-π–π stacked zippers. Two-dimensional pyridine–terpyridine π–π-stacked zippers result by synergetic and orthogonal combination of both subroutines (Scheme 4).

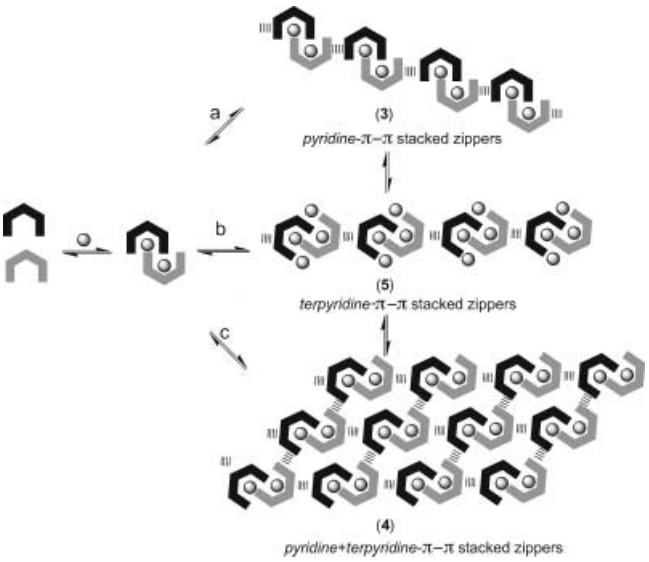

Scheme 4. a), b) One- and c) two-dimensional self-organization of π–π-stacked metallosupramolecular zippers in the solid state.

3) In terms of dynamic diversity in crystal engineering the conversion of pyridine-π–π-stacked complex **3** into terpyridine-π-π-stacked complex **5** by subsequent addition of Co^{2+} ions is reminiscent of domino series, whereby you tap on one and they all fall on succession (Figure 5).

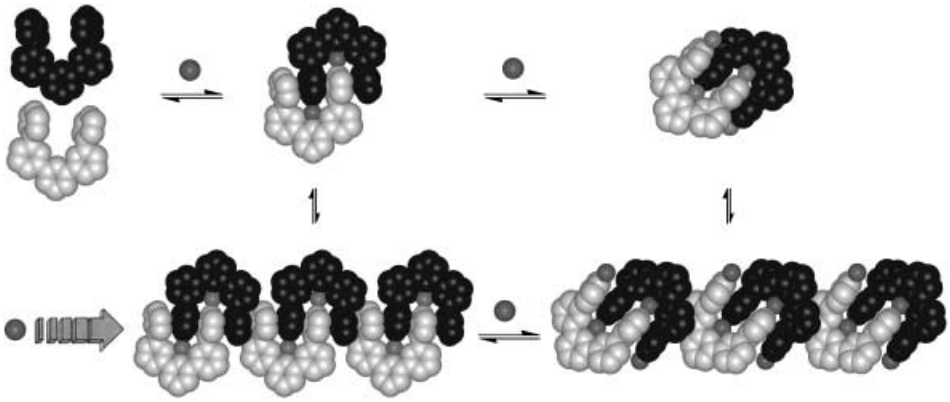

Figure 5. Dynamic diversity in the solid state, reminiscent of the dominos series principle.

Conclusion

The above results describe the controlled formation and interconversion of self-complementary duplex molecular clefts by the crossover combination of orthogonal-terpyridine and linear-pyridine metal-coordination subprograms stabilized by strong π–π stacking interactions. The robustness of these duplex cleft-type compounds results from compatibility and synergistic effect of the metal-ion binding and of the strong stacking interaction between the coordinative side arms of the components. While similar architectures has been reported in organic[14] or metallosupramolecular[12,15] systems we believe this to be the first examples of a molecular cleft stable in both solution and the solid state.

One- and two-dimensional metallosupramolecular zipper architectures are generated by further self-assembly in the solid state due to the combination of different π–π stacking subprograms. Even more remarkable is the dynamic diversity of the different multicomponent architectures in the solid state derived from the same ligand in solution. This contribution adds several new features to the systematic rationalization and prediction in metal-complex crystal engineering.

Experimental Section

General methods: All reagents were obtained from commercial suppliers and used without further purification. THF was distilled over benzophenone/Na. All organic solutions were routinely dried by using sodium sulfate (Na_2SO_4). Column chromatography was carried out on Merck alumina activity II–III. $Pb(OTf)_2$ was prepared from PbO and CF_3SO_3H as previously reported.[6c] ^1H NMR, ^{13}C NMR, COSY, and ROESY spectra were recorded on an ARX 300 MHz Bruker spectrometer in $CDCl_3$ and CD_3CN, with the use of the residual solvent peak as reference. Mass spectrometric studies were performed in the positive ion mode using a quadrupole mass spectrometer (Micromass, Platform 2+). Samples were dissolved in acetonitrile and were continuously introduced into the mass spectrometer at a flow rate of 10 mL min^{-1} through a Waters 616HPLC pump. The temperature (60 °C) and the extraction cone voltage (V_c = 5–10 V) were usually set to avoid fragmentations. Due to competitive equilibria a quantitative determination of the concentration of complexes in solution is not possible. For this reason in Figure 1 we have used MS-chromatogram peaks normalized by the maximal surface obtained for every compound. The microanalyses were carried out at Service de Microanalyses, Institut Charles Sadron, Strasbourg.

Experimental procedure for ligand 1: A solution of **7**[7] (1 g, 2 mmol) in dry THF (15 mL) was added under argon over a period of 2 h to a refluxing solution of **8** (0.5 g, 4 mmol) and *t*BuOK (0.93 g, 8.2 mmol) mmol) in dry THF (20 mL). The solution was stirred overnight at room temperature, and acetic acid (1 mL) and NH_4OAc (1 g) were added to the reaction. The mixture was refluxed for 90 min, cooled, poured into water (100 mL), extracted with chloroform (3×100 mL), washed with saturated aqueous $NaHCO_3$ (100 mL), and dried with Na_2SO_4. After evaporation the crude material was purified by flash chromatography (alumina/chloroform) to give **1** (0.6 g, 2 mmol 54%). ^{1}H NMR (250 MHz, $CDCl_3$): δ=8.78 (d, J=1.53 Hz, 2H; H_2), 8.76 (d, J=1.53 Hz, 2H; H_1), 8.66 (d, J=7.93 Hz, 2H; H_5), 8.51 (d, J=1.53 Hz, 2H; H_1'), 8.04 (t, J=7.93 Hz, 1H; H_1), 8.01 (d, J=1.53 Hz, 2H; H_2'), 7.99 (d, J=1.83 Hz, 2H; H_4), 7.65 (d, J=7.93 Hz, 2H; H_3), 3.18 (t, J=7.9 Hz, 4H; CH_2S), 1.89 (sext, J=7.9 Hz, 4H; CH_2), 1.21 ppm (t, J=7.9 Hz, 6H; CH_3); ^{13}C NMR ($CDCl_3$): δ=13.85, 22.24, 33.24, 114.16, 119.74, 122.07, 158.32, 158.34, 162.44, 162.72, 162.81 ppm; ES-MS: *m*/*z* (%): 536 (100) $[M+H]^+$; elemental analysis calcd (%) for $C_{31}H_{29}N_5S_2$ (535.7): C 69.50, H 5.46, N 13.07; found: C 68.49, H 5.36, N 13.50.

Complex 3: Formation from ligand **1** (10 mg, 18.6 mmol) and $Co(BF_4)_2{\cdot}3H_20$ (6.3 mg, 18.6 mmol) in CH_3CN at room temperature. ES-MS: *m*/*z* (%): 339 (100) $[Co_2(\mathbf{1})_2(CH_3CN)_4]^{4+}$; elemental analysis calcd (%) for $C_{68}H_{68}N_{10}S_4B_2F_8Co_2$ (1376.9): C 59.31, H 4.10, N 6.10; found: C 59.48, H 4.13, N 6.23.

Complex 4: Formation from ligand **1** (10 mg, 18,6 mmol) and $Pb(CF_3SO_3)_2$ (9.3 mg, 18.6 mmol) in CH_3CN at room temperature. ^{1}H NMR (250 MHz, $CDCl_3$): δ=8.74 (d, J=1.53 Hz, 2H; H_2), 8.76 (d, J=1.53 Hz, 2H; H_1), 8.66 (d, J=7.93 Hz, 2H; H_5), 8.51 (d, J=1.53 Hz, 2H; H_1'), 8.04 (t, J=7.93 Hz, 1H; H_1), 8.01 (d, J=1.53 Hz, 2H; H_2'), 7.99 (d, J=1.83 Hz, 2H; H_4), 7.65 (d, J=7.93 Hz, 2H; H_3), 3.18 (t, J=7.9 Hz, 4H; CH_2S), 1.89 (sext, J=7.9 Hz, 4H; CH_2), 1.21 (t, J=7.9 Hz, 6H; CH_3); ES-MS: *m*/*z* (%): 892 (100) $[Pb_2(\mathbf{1})_2(CF_3SO_3)_2]^{2+}$; elemental analysis calcd (%) for $C_{64}H_{56}N_{12}S_{12}O_{12}F_{12}Pb_2$ (2212.8): C 34.74, H 2.55, N 7.60; found: C 34.58, H 2.67, N 7.64.

Complex 5: Formation from ligand **1** (10 mg, 18.6 mmol) and $Co(BF_4)_2{\cdot}3H_20$ (12.6 mg, 37.3 mmol) in CH_3CN at room temperature. ES-MS: *m*/*z* (%): 310 (100) $[Co_4(\mathbf{1})_2(CH_3CN)_{14}(BF_4)_4]^{4+}$; elemental analysis calcd (%) for $C_{68}H_{68}N_{10}S_4B_2F_8Co_2$ (2345.9): C 46.61, H 2.95, N 8.37; found: C 46.58, H 2.83, N 8.33.

Complex 6: Formation from ligand **1** (10 mg, 18.6 mmol) and and $Pb(CF_3SO_3)_2$ (18.6 mg, 37.3 mmol) in CH_3CN at room temperature. ^{1}H NMR (250 MHz, $CDCl_3$): δ=8.78 (d, J=1.53 Hz, 2H; H_2), 8.76 (d, J=1.53 Hz, 2H; H_1), 8.66 (d, J=7.93 Hz, 2H; H_5), 8.51 (d, J=1.53 Hz, 2H; H_1'), 8.04 (t, J=7.93 Hz, 1H; H_1), 8.01 (d, J=1.53 Hz, 2H; H_2'), 7.99 (d, J=1.83 Hz, 2H; H_4), 7.65 (d, J=7.93 Hz, 2H; H_3), 3.18 (t, J=7.9 Hz, 4H; CH_2S), 1.89 (sext, J=7.9 Hz, 4H; CH_2), 1.21 (t, J=7.9 Hz, 6H; CH_3); ES-MS: *m*/*z* (%): 480 (100) $[Pb_4(\mathbf{1})_2(CF_3SO_3)_4(CH_3CN)_4]^{4+}$; elemental analysis calcd (%) for $C_{68}H_{56}N_{12}S_{16}O_{24}F_{24}Pb_2$ (2808.66): C 29.08, H 2.01, N 5.98; found: C 29.28, H 2.33, N 6.00.

X-ray crystallographic data for complexes 3, 4, and 5: X-ray diffraction data measurements for **3**–**5** were carried out at beamline ID11 at the European Synchrotron Facility (ESRF) at Grenoble. Wavelengths of 0.50915 Å (compound **3**) or 0.32826 Å (**4** and **5**) and were selected using a double crystal Si(111) monochromator. Crystals were placed in oil, mounted on a glass fiber and placed in a low-temperature N_2 stream. Data were collected using a Bruker "Smart" CDD camera system at fixed 2θ and reduced using the Bruker SAINT software. The structures determination and refinement were carried out with SHELXS[16] and SHELXL[17] respectively. All non-hydrogen atoms were refined anisotropically; hydrogen atoms were included at calculated positions by using a riding model.

Single crystals of **3**, $[C_{72}H_{73}AgB_4CoF_6N_{12}O_6S_6]$ were grown from acetonitrile/benzene (1:1) at room temperature. Measurement was carried out on a single pink crystal of dimension 0.04×0.02×0.01 mm. The unit cell was triclinic with space group of $P\bar{1}$. Cell dimensions were a=11.328(3), b=13.692(3), c=14.175(4) Å, α=102.495(14), β=91.008(13), γ=108.753(11)°, V=2023.6(8) Å^3, Z=1. Of the 12468 reflections collected from 8.92°≤θ≤14.01°, 4775 were unique and 4424 were observed with $I>2\sigma(I)$. . The final number of parameters and constraints (on relative anisotropic displacement factors) were 534 and 146. Final R factors were R_1=0.0511 and wR_2=0.1301, (all observed data), R_1=0.0480 and wR_2=0.1275 [$I>4\sigma(I)$], minimum and maximal residual electron densities were −0.544 and 0.772 e Å^{-3}.

Single crystals of **4**, $[C_{39}H_{37}F_6N_5O_6PbS_4]$ were grown from acetonitrile/benzene (1:1) at room temperature. Measurement was carried out on a single pink crystal of dimension of a single yellow crystal of dimensions 0.10×0.05×0.04 mm. The unit cell was triclinic with space group of $P\bar{1}$. Cell dimensions were a=12.6220(5), b=13.1936(5), c=14.8022(4) Å, α=69.773(1), β=88.406(1), γ=67.549(2)°, V=2122.19(13) Å^3, Z=2. Of the 12468 reflections collected from 8.92°≤θ≤14.01°, 6028 were unique and 5887 were observed with $I>2\sigma(I)$. Structure solution and refinement were carried out as for **4**. The final number of parameters was 533. Final R factors were R_1=0.0151 and wR_2=0.0367, (all observed data), R_1=0.0145 and wR_2=0.0363 [$I>4\sigma(I)$], minimum and maximal residual electron densities were −0.35 and 0.36 e Å^{-3}.

Single crystals of **5**, $[C_{31}H_{29}BCo_2F_4N_5OS_2]$ were grown from acetonitrile/benzene (1:1) at room temperature. Measurement was carried out on a single red crystal of dimension 0.09×0.05×0.04 mm. The unit cell was triclinic with space group $P\bar{1}$. Cell dimensions were a=13.5860(3), b=15.1551(3), c=16.2527(3) Å, α=112.763(1), β=97.167(1), γ=107.431(1)°, V=2831.74(10) Å^3, Z=4. Of the 20852 reflections collected from 9.27°≤θ≤14.97°, 9832 were unique and 9245 were observed with $I>2\sigma(I)$. The final number of parameters was 836. Final R factors were R_1=0.0454 and wR_2=0.1221, (all observed data), R_1=0.0434 and wR_2=0.1200 [$I>4\sigma(I)$], minimum and maximal residual electron densities were −0.480 and 0.882 e Å^{-3}.

CCDC-227293 (**3**), CCDC-227294 (**4**), and CCDC-227295 (**5**) contain the supplementary crystallographic data for this paper. These data can be obtained free of charge via www.ccdc.cam.ac.uk/conts/retrieving.html (or from the Cambridge Crystallographic Data Centre, 12 Union Road, Cambridge CB21EZ, UK; fax: (+44)1223-336-033; or deposit@ccdc.cam.uk).

Acknowledgment

This research was supported by the Ministère de la Recherche et de la Technologie, ACI Jeunes Chercheurs—4034, 2002, ESRF and by the CNRS.

[1] a) J.-M. Lehn, *Proc. Natl. Acad. Sci. USA* **2002**, *99*, 4763–4768; b) J.-M. Lehn, *Chem. Eur. J.* **2000**, *6*, 2097–2102; c) J.-M. Lehn, in *Supramolecular Polymers*, (Ed.: A. Ciferi), Dekker, New York, NY, **2000**, pp. 615–641.

[2] For recent reviews on metal ion metal self-assembly, see for example: a) S. Leininger, B. Olenyuk, P. J. Stang, *Chem. Rev.* **2000**, *100*, 853–908; b) G. F. Swiegers, T. F. Malfetese, *Chem. Rev.* **2000**, *100*, 3483–3538; c) B. J. Holliday, C. A. Mirkin, *Angew. Chem.* **2001**, *113*, 2076–2097; *Angew. Chem. Int. Ed.* **2001**, *40*, 2022–2043; d) S. R. Seidel, P. J. Stang, *Acc. Chem. Res.* **2002**, *35*, 972–983; e) M. Fujita, K. Umemoto, M. Yoshizawa, N. Fujita, T. Kusukawa, K. Biradha, *Chem. Commun.* **2001**, 509–518.

[3] D. P. Funeriu, K. Rissanen, J.-M. Lehn, *Proc. Natl. Acad. Sci. USA* **2001**, *98*, 10546–10551, and references therein.

[4] M. L. Scudder, H. A. Goodwin, I. G. Dance, *New J. Chem.* **1999**, *23*, 695–705.

[5] J. Y. Lu, C. Norman, K. A. Abboud, A. Ison, *Inorg. Chem. Commun.* **2001**, *4*, 459–461.

[6] a) M. Ruben, E. Breuning, J.-P. Gisselbrecht, J.-M. Lehn, *Angew. Chem.* **2000**, *112*, 4312–4315; *Angew. Chem. Int. Ed.* **2000**, *39*, 4139–4142; b) E. Breuning, G. S. Hanan, F. J. Romero-Salguero, A. M. Garcia, P. N. W. Baxter, J.-M. Lehn, E. Wegelius, K. Rissanen, H. Nierengarten, A. van Dorsselaer, *Chem. Eur. J.* **2002**, *8*, 3458–3466c) M. Barboiu, G. Vaughan, R. Graff, J.-M. Lehn, *J. Am. Chem. Soc.* **2003**, *125*, 10257–10265.

[7] K. T. Potts, K. A. Gheysen-Raiford, K. M. Keshavarz, *J. Am. Chem. Soc.* **1993**, *115*, 2793–2807.

[8] For *transoid--transoid* confomation definition see: M. Barboiu, J.-M. Lehn, *Proc. Natl. Acad. Sci. USA* **2002**, *99*, 5201–5206.

[9] a) A. Marquis, J.-P. Kintzinger, R. Graff, P. N. W. Baxter, J.-M. Lehn, *Angew. Chem.* **2002**, *114*, 2884–2888; *Angew. Chem. Int. Ed.* **2002**, *41*, 2760–2764; b) S. Hiraoka, T. Yi, M. Shiro, M. Shionoya, *J. Am. Chem. Soc.* **2002**, *124*, 14510–14511.
[10] P. N. W. Baxter, R. G. Khoury, J.-M. Lehn, G. Baum, D. Fenske, *Chem. Eur. J.* **2000**, *6*, 4140–4148.
[11] a) C. Janiak, *J. Chem. Soc. Dalton Trans.* **2000**, 3885–3896; b) M. Barboiu, G. Vaughan, N. Kyritsakas, J.-M. Lehn, *Chem. Eur J.* **2003**, *9*, 763–769.
[12] D. A. McMorran, P. A. Stell, *Chem. Commun.* **2002**, 2120–2121.
[13] For a comment, see reference [1], p. 199–201.
[14] a) J. N. H. Reek, J. A. A. W. Elemans, R. Gelder, P. T. Beurskens, A. E. Rowan, R. J. M. Nolte , *Tetrahedron* **2003**, *59*, 175–185; b) Q. Z. Zhou, X. K. Jiang, X. B. Shao, G. J. Chen, M. X. Jia, Z. T. Li, *Org. Lett.* **2003**, *5*, 1955–1958; c) A. P. Bisson, F. J. Carver, D. S. Eggleston, R. C. Haltiwanger, C. A. Hunter, D. L. Livinstone, J. F. McCabe, C. Rotger, A. E. Rowan, *J. Am. Chem. Soc.* **2000**, *122*, 8856–8868.
[15] a) X. M. Chen, G. F. Liu, *Chem. Eur. J.* **2002**, *8*, 4811–4817; b) Y. Q. Zheng, J. Sun, J. L. Lin, *Z. Anorg. Allg. Chem.* **2000**, *626*, 1501–1504; c) B.H Ye, X. M. Chen, G. Q. Xue, L. N. Ji, *J. Chem. Soc. Dalton Trans.* **1998**, 2827–2831.
[16] G. M. Sheldrick, SHLXS97, A Program for Automatic Solution of Crystal Structures, University of Göttingen, Germany, **1997**.
[17] G. M. Sheldrick, SHLXL97, A Program for Automatic Refinement of Crystal Structures, University of Göttingen, Germany, **1997**.

Received: November 26, 2003 [F5750]